Chem. Mater. **1998,** *10,* 3131−3139

The First Fully Fluorinated Organically Templated Materials: Synthesis, Structures, and Physical Properties of $[H_3N(CH_2)_3NH_3]U_2F_{10}\cdot 2H_2O$, $[H_3N(CH_2)_4NH_3]U_2F_{10}\cdot 3H_2O$, $[H_3N(CH_2)_6NH_3]U_2F_{10}\cdot 2H_2O$, and $[HN(CH_2CH_2NH_3)_3]U_5F_{24}$

Robin J. Francis,† P. Shiv Halasyamani, and Dermot O'Hare*

Inorganic Chemistry Laboratory, University of Oxford, South Parks Road,
Oxford, UK OX1 3QR

Received April 1, 1998. Revised Manuscript Received June 22, 1998

A series of new layered uranium(IV) fluorides have been prepared under hydrothermal conditions from UO_2, HF, and H_3PO_4 by using $H_2N(CH_2)_nNH_2$ (n = 3, 4, or 6), and $N(CH_2CH_2NH_2)_3$ as structure-directing agents. $[H_3N(CH_2)_3NH_3]U_2F_{10}\cdot 2H_2O$ (UFO-1), $[H_3N(CH_2)_4NH_3]U_2F_{10}\cdot 3H_2O$ (UFO-2), $[H_3N(CH_2)_6NH_3]U_2F_{10}\cdot 2H_2O$ (UFO-3), and $[HN(CH_2CH_2NH_3)_3]U_5F_{24}$ (UFO-4) have been characterized by single-crystal X-ray diffraction, thermogravimetric analysis, BET isotherms, and magnetic susceptibility measurements. UFO-1, 2, 3, and 4 contain negatively charged uranium fluoride (UF) layers constructed from linked UF_n polyhedra separated by charge balancing organic cations and occluded water molecules. In UFO-1, 2, and 3, the layers are constructed from equivalent UF_9 tricapped trigonal prisms that share three edges and two corners, whereas UFO-4 contains both UF_8 bicapped trigonal prisms and UF_9 tricapped trigonal prisms. We have demonstrated that the interlamellar organic cations in these materials can be ion-exchanged with a large variety of alkali, alkaline earth, and transition metal cations, thus providing a low-temperature route to new condensed mixed metal uranium fluorides. The magnetic susceptibility data indicate that UFO-1, 2, and 3 exhibit Curie-Wiess behavior between room temperature and 20 K. [Crystal data: UFO-1, monoclinic, space group $P2_1/c$ (no. 14), $a = 10.715(1)$ Å, $b = 7.097(1)$ Å, $c = 8.767(1)$ Å, $\beta = 93.804(6)°$, $V = 665.21(1)$ Å^3 (T = 150 K), $Z = 2$, $R(F) = 5.42\%$, $R_w(F) = 6.79\%$; UFO-2, triclinic, space group $P\bar{1}$ (no. 2), $a = 12.024(2)$ Å, $b = 7.149(3)$ Å, $c = 8.765(2)$ Å, $\alpha = 90.063(4)°$, $\beta = 107.133(5)°$, $\gamma = 92.098(3)°$, $V = 719.49(3)$ Å^3 (T = 150 K), $Z = 2$, $R(F) = 8.05\%$, $R_w(F) = 10.11\%$; UFO-3, monoclinic, space group $P2_1/c$ (no. 14), $a = 13.800(2)$ Å, $b = 7.056(1)$ Å, $c = 8.720(1)$ Å, $\beta = 108.338(6)°$, $V = 805.97(2)$ Å^3 (T = 150 K), $Z = 2$, $R(F) = 3.64\%$, $R_w(F) = 4.65\%$; UFO-4, triclinic, space group $P\bar{1}$ (no. 2), $a = 11.534(2)$ Å, $b = 11.532(4)$ Å, $c = 9.634(2)$ Å, $\alpha = 104.034(4)°$, $\beta = 101.112(8)°$, $\gamma = 93.922(4)°$, $V = 1210.9(5)$ Å^3 (T = 150 K), $Z = 2$, $R(F) = 6.12\%$, $R_w(F) = 8.19\%$.]

Introduction

Hydrothermal crystallization in the presence of cationic organic species has been demonstrated to be a versatile technique for the synthesis of new materials with novel structural architecture.[1] By careful control of the synthesis conditions and the organic species employed it is possible to synthesize a vast range of open-framework and layered materials in which a cationic organic species is occluded within an anionic inorganic framework. Of central importance is the ability of the organic molecules to profoundly influence the structure of the synthesized product, and to 'direct' the formation of materials with particular structural and physical properties.[2,3] In aluminosilicate and metal phosphate chemistry, the ability of organic molecules to 'template' the formation of particular structures is a well-established concept,[4−6] although the degree to which the final structures reflect the structural properties of the organic species varies greatly, and the details of the templating process are open to much debate.[7] Nevertheless, the exquisite control over the detailed

---

† Current address: Department of Chemistry, University of Houston, 4800 Calhoun, Houston, TX 77204-5641.

(1) See, for example: (a) Estermann, M.; McCusker, L. B.; Baerlocher, C.; Merrouche, A.; Kessler, H. *Nature* **1991**, *352*, 320. (b) Haushalter, R. C.; Mundi, L. A. *Chem. Mater.* **1992**, *4*, 31. (c) Jones, R. H.; Thomas, J. M.; Chen, J.; Xu, R.; Huo, Q.; Li, S.; Ma, Z.; Chippindale, A. M. *J. Solid State Chem.* **1993**, *102*, 204. (d) Loiseau, T.; Ferey, G. *J. Solid State Chem.* **1994**, *111*, 403. (e) Loiseau, T.; Ferey, G. *J. Solid State Chem.* **1994**, *111*, 416. (f) Lobo, R. F.; Davis, M. E. *J. Am. Chem. Soc.* **1995**, *117*, 3766. (g) Freyhardt, C. C.; Tsapatsis, M.; Lobo, R. F.; Balkus, K. J., Jr.; Davis, M. E. *Nature* **1996**, *381*, 295. (h) Harrison, W. T. A.; Phillips, M. L. F. *Chem. Mater.* **1997**, *9*, 1837. (i) Stalder, S. M.; Wilkinson, A. P. *Chem. Mater.* **1997**, *9*, 2168.

(2) Lok, B. M.; Cannon, T. R.; Messina, C. A. *Zeolites* **1983**, *3*, 282.

(3) Gies, H.; Marler, B. *Zeolites* **1992**, *12*, 42.

(4) Barrer, R. M. *Hydrothermal Chemistry of Zeolites*; Academic: London, 1982.

(5) Breck, D. W. *Zeolite Molecule Sieves: Structure, Chemistry and Use*; Wiley and Sons: London, 1974.

(6) Szostak, R. *Molecular Sieves: Principles of Synthesis and Identification*; Van Nostrand Reinhold: New York, 1989.

(7) Davis, M. E.; Lobo, R. F. *Chem. Mater.* **1992**, *4*, 756.

10.1021/cm980225x CCC: $15.00

topology of the anionic framework that can be achieved by alteration of the steric and electronic properties of the organic has been exploited by chemists to synthesize materials with an astonishingly diverse range of structural characteristics. Aside from the purely academic interest in these fascinating reactions, the range of materials chemistry applications, including heterogeneous catalysis,[8] molecular sieving, and ion-exchange,[9] for which these materials are suitable has led to continued interest in the synthesis of new hybrid inorganic/organic layered and microporous materials. Although to date the vast majority of examples have been derived from main group elements, such as silicon, aluminum, and phosphorus,[7,10,11] a wide variety of other main group and transition metals have recently been incorporated into three-dimensional and layered framework structures.[12-40] Such materials are of interest for two primary reasons. First, the ability of some main group and transition metals to exist in five, six, seven or higher coordination environments, as opposed to zeolites and aluminophosphates that only contain tetrahedrally coordinated units, allows the synthesis of new more complex framework architectures. Second, the incorporation of transition metals that are capable of existing in a variety of different oxidation states within an open-framework structure offers the possibility of combining the size and shape-selectivity demonstrated by framework materials with the catalytic, magnetic, and photochemical properties associated with d-block elements. Metals that have been incorporated into layered and microporous frameworks via hydrothermal crystallizations in the presence of organic 'templating' agents include Be,[12] Ga,[13-17] In,[18] Mo,[19] V,[20-24] Zn,[25-28] Co,[29-32] and Fe.[33-40]

To date, however, with the exception of two uranium(VI) phosphate phases that we recently reported,[41] we are not aware of any syntheses of hybrid organic/inorganic materials in which actinide elements such as uranium are incorporated into layered or microporous frameworks. We are interested in exploring the synthesis of these materials for a number of reasons. First, given the high coordination numbers and the variety of coordination geometries adopted by actinide elements, hydrothermal crystallizations in the presence of bulky organic cations could be expected to result in the formation of new, complex framework architectures. Clearfield and co-workers have demonstrated that in the synthesis of uranyl phosphonates, the presence of sterically demanding organic groups on the phosphonate ligands leads to the formation of novel structure types, including porous structures.[42-46] Second, these materials may be envisioned to exhibit useful catalytic, ion-exchange, and intercalation properties. For example, hydrogen uranyl phosphate (HUP) is a fast hydrogen ion conductor and a versatile ion-exchange reagent,[47-50] and Hutchings et al. recently demonstrated that uranium oxide-based materials are effective oxidation catalysts for the destruction of a range of hydrocarbon- and chlorine-containing industrial pollutants.[51] Finally, the existence of a number of stable oxidation states of actinides, such as uranium, offers the possibility of synthesising materials with useful optical and magnetic properties.

The addition of fluoride ions as a mineralizing agent in hydrothermal syntheses has been shown to be an effective method for the synthesis of novel structure types.[52-54] The fluorine appears to play a role both in aiding the crystallization of the final phase and in stabilizing the increased coordination of the metal atoms, thus leading to structures with new and more

---

(8) Venuto, P. B. *Microporous Mater.* **1994**, *2*, 297.
(9) Clearfield, A. *Chem. Rev.* **1988**, *88*, 125.
(10) Wilson, S. T.; Lok, B. M.; Messina, C. A.; Cannon, T. R.; Flanigen, E. M. *ACS Symp. Ser.* **1983**, *218*, 79.
(11) Flanigen, E. M.; Patton, R. L.; Wilson, S. T. *Stud. Surf. Sci. Catal.* **1988**, *37*, 13.
(12) Gier, T. E.; Stucky, G. D. *Nature* **1991**, *349*, 508.
(13) Loiseau, T.; Ferey, G. *J. Chem. Soc., Chem. Commun.* **1992**, 1197.
(14) Loiseau, T.; Ferey, G. *J. Solid State Chem.* **1994**, *111*, 403.
(15) Loiseau, T.; Ferey, G. *J. Mater. Chem.* **1996**, *6*, 1073.
(16) Loiseau, T.; Retoux, R.; Lacorre, P.; Ferey, G. *J. Solid State Chem.* **1994**, *111*, 427.
(17) Ferey, G. *J. Fluor. Chem.* **1995**, *72*, 187.
(18) Chippindale, A. M.; Brech, S. J.; Cowley, A. R.; Simpson, W. M. *Chem. Mater.* **1996**, *8*, 2259.
(19) Haushalter, R. C.; Mundi, L. A. *Chem. Mater* **1992**, *4*, 31.
(20) Khan, M. I.; Meyer, L. M.; Haushalter, R. C.; Schweitzer, A. L.; Zubieta, J.; Dye, J. L. *Chem. Mater.* **1996**, *8*, 43.
(21) Riou, D.; Ferey, G. *J. Solid State Chem.* **1994**, *111*, 422.
(22) Riou, D.; Ferey, G. *Eur. J. Solid State Inorg. Chem.* **1994**, *31*, 605.
(23) Soghomonian, V.; Chen, Q.; Haushalter, R. C.; Zubieta, J.; O'Conner, C. J.; Lee, Y.-S. *Chem. Mater.* **1993**, *5*, 1690.
(24) Soghomonian, V.; Chen, Q.; Haushalter, R. C.; Zubieta, J. *Chem. Mater.* **1993**, *5*, 1595.
(25) Annen, M. J.; Davis, M. E.; Higgins, J. B.; Schlenker, J. L. *J. Chem. Soc., Chem. Commun.* **1991**, 1175.
(26) Gier, T. E.; Stucky, G. D. *Nature* **1991**, *349*, 508.
(27) Harrison, W. T. A.; Broach, R. W.; Bedard, R. A.; Gier, T. E.; Bu, X.; Stucky, G. D. *Chem. Mater.* **1996**, *8*, 691.
(28) Harrison, W. T. A.; Phillips, M. L. F. *Chem. Mater.* **1997**, *9*, 1837.
(29) Chippindale, A. M.; Walton, R. I. *J. Chem. Soc., Chem. Commun.* **1994**, 2453.
(30) Chippindale, A. M.; Cowley, A. R. *Zeolites* **1997**, *18*, 176.
(31) DeBord, J. R. D.; Haushalter, R. C.; Zubieta, J. *J. Solid State Chem.* **1996**, *125*, 270.
(32) Feng, P. Y.; Bu, X. H.; Stucky, G. D. *Nature* **1997**, *388*, 735.
(33) Riou, D.; Cavellec, M.; Ferey, G. *Acta Crystallogr.* **1994**, *C50*, 1379.
(34) Cavellec, M.; Riou, D.; Ferey, G. *J. Solid State Chem.* **1994**, *112*, 441.
(35) Cavellec, M.; Riou, D.; Ninclaus, C.; Greneche, J. M.; Ferey, G. *Zeolites* **1996**, *17*, 250.
(36) Cavellec, M.; Riou, D.; Greneche, J. M.; Ferey, G. *Microporous Mater.* **1997**, *8*, 103.
(37) Cavellec, M.; Riou, D.; Greneche, J. M.; Ferey, G. *Inorg. Chem.* **1997**, *36*, 2187.
(38) Lii, K. H. *J. Chem. Soc., Dalton Trans.* **1996**, 819.
(39) Lii, K. H.; Huang, Y. F. *Chem. Commun.* **1997**, 839.
(40) Lii, K. H.; Wang, S. L. *J. Solid State Chem.* **1997**, *128*, 21.
(41) Francis, R. J.; Drewitt, M. J.; Halasyamani, P. S.; Ranganathachar, C.; O'Hare, D.; Clegg, W.; Teat, S. J. *Chem. Commun.* **1998**, 279.
(42) Grohol, D.; Subramanian, M. A.; Poojary, D. M.; Clearfield, A. *Inorg. Chem.* **1996**, *35*, 5264.
(43) Grohol, D.; Clearfield, A. *Abstracts Of Papers Of The American Chemical Society* **1997**, *213*, 841.
(44) Poojary, D. M.; Grohol, D.; Clearfield, A. *Angew. Chem., Int. Ed. Engl.* **1995**, *34*, 1508.
(45) Poojary, D. M.; Grohol, D.; Clearfield, A. *J. Phys. Chem. Solids* **1995**, *56*, 1383.
(46) Poojary, D. M.; Cabeza, A.; Aranda, M. A. G.; Bruque, S.; Clearfield, A. *Inorg. Chem.* **1996**, *35*, 1468.
(47) Grohol, D.; Blinn, E. L. *Inorg. Chem.* **1997**, *36*, 3422.
(48) Johnson, C. H.; Shilton, M. G.; Howe, A. T. *J. Solid State Chem.* **1981**, *37*, 37.
(49) Moreno-Real, L.; Pozas-Tormo, R.; Martinez-Lara, M.; Bruque-Gamez, S. *Mater. Res. Bull.* **1987**, *22*, 19.
(50) Pozas-Tormo, R.; Moreno-Real, L.; Martinez-Lara, M.; Rodriguez-Castellon, E. *Can. J. Chem.* **1986**, *64*, 35.
(51) Hutchings, G. J.; Heneghan, C. S.; Hudson, I. D.; Taylor, S. H. *Nature* **1996**, *384*, 341.
(52) Guth, J. L.; Kessler, H.; Wey, R. *Stud. Surf. Sci. Catal.* **1986**, *28*, 121.
(53) Guth, J. L.; Kessler, H.; Higel, J. M.; Lamblin, J. M.; Patarin, J.; Sieve, A.; Chezcau, J. M.; Wey, R. *ACS Symp. Ser.* **1989**, *398*, 176.
(54) Kessler, H. *MRS Symp. Ser.* **1991**, *233*, 47.

complex framework architecture. The use of fluoride has been particularly successful for the synthesis of novel gallium phosphate microporous materials such as cloverite,[55] ULM-5,[14] and the recently reported TREN−GaPO.[56] We have been exploring the hydrothermal synthesis of new uranium-based materials in the presence of both organic molecules and the fluoride ion, and we report here the synthesis, characterization and physical properties of $[H_3N(CH_2)_3NH_3]U_2F_{10}\cdot 2H_2O$, $[H_3N(CH_2)_4NH_3]U_2F_{10}\cdot 3H_2O$, $[H_3N(CH_2)_6NH_3]U_2F_{10}\cdot 2H_2O$, and $[HN(CH_2CH_2NH_3)_3]U_5F_{24}$, novel uranium(IV) fluoride phases synthesized via hydrothermal crystallization in the presence of organic cations. We denote these materials UFO-1−4 (for uranium fluoride materials synthesized in Oxford numbers 1 to 4), respectively.

Experimental Section

Synthesis. UFO-1, 2, and 3 were synthesized by the reaction of UO_2, H_3PO_4, HF, $H_2N(CH_2)_nNH_2$ (where $n = 3$, 4, or 6), and H_2O in the mole ratio 3:32:32:8:650 under hydrothermal conditions at 180 °C for 1 day, followed by slow cooling at 6 °C/h to room temperature. UFO-4 was synthesized by the reaction of U_3O_8, H_3PO_4, HF, $N(CH_2CH_2NH_2)_3$, and H_2O in the mole ratio 1:48:48:8:650 at 180 °C for 1 day, followed by slow cooling at 6 °C/h to room temperature. All syntheses were performed in Teflon-lined stainless steel autoclaves under autogenous pressures. Fill volumes of ~25% were used. For all reactions, the required volume of water was added to the solid uranium oxide, followed sequentially by the phosphoric acid (85% solution), hydrofluoric acid (40% solution), and organic template. Depleted uranium oxide, phosphoric acid, and the organic templates were obtained from British Nuclear Fuels Ltd., BDH, and Aldrich, respectively. After reaction, the products were recovered by filtration, washed with water, and allowed to dry in air. This procedure yielded pure monophasic, bright green, rhomboid-shaped single crystals of UFO-1, 2, and 3 in yields of ~70%, based on UO_2. UFO-4 formed as large, very dark green crystals, together with some impurity phases. Despite the use of phosphoric acid in the reactions, no phosphate was found in the final products. However, attempts to make these materials in the absence of phosphoric acid were unsuccessful. It seems likely that the phosphoric acid is playing a necessary role in modifying the pH of the reaction mixture. Elemental analyses of all three compounds, including fluorine analyses,[57] confirmed the absence of phosphorus in the materials and the correctness of the given formulas. Elemental analyses: found (calcd) for UFO-1: C% 4.44 (4.63), H% 2.05 (2.07), N% 3.43 (3.60), U% 62.19 (61.17), F% 24.20 (24.41); found (calcd) for UFO-2: C% 5.86 (5.93), H% 2.19 (2.59), N% 3.29 (3.46), U% 56.73 (58.75), F% 23.56 (23.50); found (calcd) for UFO-3: C% 7.94 (8.79), H% 2.56 (2.70), N% 3.10 (3.42), U% 56.35 (58.04), F% 22.92 (23.17).

Crystallography. All crystallographic data were acquired using graphite-monochromated Mo Kα radiation ($\lambda = 0.71073$ Å) on an image-plate Enraf-Nonius DIP 2000 diffractometer at a step of 2° per frame ($\theta_{max} = 26°$). The crystals were mounted on a fiber under paratone oil and cooled on the diffractometer. Each frame was collected, indexed, and processed using DENZO, and the files scaled together using SCALEPACK to produce the *hkl* file.[58] For all structures, the heavy atom positions were determined by direct methods using SIR92.[59] Subsequent Fourier-difference syntheses revealed the positions of the remaining non-hydrogen atoms. All uranium atoms were refined with anisotropic thermal parameters using full-matrix least-squares procedures on *F*. In general, all other atoms were refined using isotropic temperature factors, although in certain cases, anisotropic temperature factors were refined on other non-hydrogen atoms. Hydrogen atoms were fixed in geometrically idealized positions and allowed to ride on their attached carbon atoms with isotropic thermal parameters according to the atom to which they were connected (these were not refined). Corrections were made for Lorentz and polarization effects.[60] An empirical data correction using DIFABS was also applied.[61] A Chebyshev weighting scheme[62] was applied in the refinement of the structure, the data in all cases being corrected for the effects of anomalous dispersion and isotropic extinction (via an overall extinction parameter)[63] in the final stages of refinement. All crystallographic calculations were performed using the Oxford CRYSTALS system[64] running on a Silicon Graphics Indigo R4000 computer.

In UFO-1, the $[H_3N(CH_2)_3NH_3]^{2+}$ cation lies on an inversion center with the central carbon located on the special crystallographic position. Each of the end carbon atoms is disordered around this position. This disorder was modeled by placing a carbon atom on two sites, each with an occupancy of 0.5, and applying soft constraints to the relevant bond lengths. No such problem arose in UFO-2 because of the lower symmetry of the structure. In UFO-3, the organic cation is again centered on the 2-fold axis, but in this case the crystallographic special position is located in the middle of central carbon−carbon bond and no disorder is observed.

Thermal Analysis. Thermogravimetric analysis (TGA) was performed using a Rheometric Scientific STA 1500H thermal analyzer. Samples weighing ~20 mg were contained within platinum crucibles and introduced to the apparatus. Samples were heated at a rate of 5 °C/min from room temperature to ~900 °C under either a static atmosphere of air or a gas flow of nitrogen supplied from a cylinder.

Brunauer−Emmett−Teller (BET) Measurements. BET measurements were performed on 0.1 g of ground samples of UFO-1−3 using an experimental apparatus described earlier.[65] Measurements were performed at pressures of N_2 from 0.05 bar up to a maximum of 0.4 bar at intervals of 0.05 bar. Measurements were performed at both room temperature and 180 °C. Surface areas of ~20 m^2/g were found in all cases.

Ion-Exchange Experiments. Ion-exchange reactions were performed by stirring ~20 mg of the compound in 5 mL of a 2 M aqueous solution of the appropriate metal salt at either room temperature or 70 °C for a 1−4-day period. Metals used were Na^+, K^+, Cs^+, Mn^{2+}, Fe^{2+}, Co^{2+}, Ni^{2+}, and Cu^{2+}. Specifically, Na^+, K^+, and Cs^+ exchanges were performed by stirring the bromide salt at room temperature for 48 h. The Mn^{2+}, Fe^{2+}, Co^{2+}, Ni^{2+}, and Cu^{2+} exchange were performed by stirring the acetate salts at 70 °C for 1 day. Complete exchange was achieved for Na^+, K^+, Cs^+, and Co^{2+}, whereas only partial exchange was observed for Mn^{2+}, Fe^{2+}, Ni^{2+}, and Cu^{2+}. Complete exchange was confirmed by the absence of host 100 reflections and the absence of carbon or nitrogen in the exchanged products. Although, detailed experiments on the relative ion-exchange affinities were not performed, in general, alkali metal cations were more readily exchanged than transition metal cations, and any individual cation could be more readily exchanged into UFO-3 than UFO-2 or UFO-1. The

---

(55) Estermann, M.; McCusker, L. B.; Baerlocher, C.; Merrouche, A.; Kessler, H. *Nature* **1991**, *352*, 320.

(56) Weigel, S. J.; Weston, S. C.; Cheetham, A. K.; Stucky, G. D. *Chem. Mater.* **1997**, *9*, 1293.

(57) Fluorine analysis was performed by Analytische Laboratorien, Industriepark Kaiserau, D-51789 Lindlar, Germany.

(58) Otwinowski, Z. *Data Collection and Processing, Proceedings of the CCP4 Study Weekend*, Daresbury Laboratory, Warrington, 1993.

(59) Altomare, A.; Cascarano, G.; Giacovazzo, C.; Guagliardi, A.; Ploidori, G.; Burla, M. C.; Carnalli, M. *J. Appl. Crystallogr.* **1994**, *27*, 435.

(60) North, A. C. T.; Phillips, D. C.; Matthews, F. S. *Acta Crystallogr.* **1968**, *A24*, 351.

(61) Walker, N.; Stuart, D. *Acta Crystallogr.* **1983**, *A39*, 159.

(62) Carruthers, J. R.; Watkin, D. W. *Acta Crystallogr.* **1979**, *A35*, 698.

(63) Larson, A. C. *Acta Crystallogr.* **1967**, *23*, 664.

(64) Carruthers, J. R.; Watkin, D. J. *CRYSTALS User Manual*, Oxford University Computing Centre, Oxford, 1975.

(65) York, A. Ph.D. Thesis, Oxford University, 1993.

Table 1. Selected Crystallographic Data for the Organically Templated Uranium(IV) Fluorides $(H_3N(CH_2)_3NH_3)U_2F_{10}\cdot 2H_2O$ (UFO-1), $(H_3N(CH_2)_4NH_3)U_2F_{10}\cdot 3H_2O$ (UFO-2), $(H_3N(CH_2)_6NH_3)U_2F_{10}\cdot 2H_2O$ (UFO-3), and $(HN(CH_2CH_2NH_3)_3)U_5F_{24}$ (UFO-4)

	UFO-			
parameter	1	2	3	4
chemical formula	$C_3H_{16}U_2F_{10}N_2O_2$	$C_4H_{20}U_2F_{10}N_2O_3$	$C_6H_{22}U_2F_{10}N_2O_2$	$C_6H_{22}U_5F_{24}N_4$
formula weight	778.21	810.26	820.29	1796.37
a (Å)	10.715(1)	12.024(2)	13.800(2)	11.534(2)
b (Å)	7.097(1)	7.149(3)	7.056(2)	11.532(4)
c (Å)	8.767(1)	8.765(2)	8.720(3)	9.634(2)
α (deg)	90	90.063(4)	90	104.034(4)
β (deg)	93.804(6)	107.133(5)	108.338	101.112(8)
γ (deg)	90	92.098(3)	90	93.922(4)
V (Å^3)	665.21(1)	719.49(3)	805.97(2)	1210.9(5)
Z	2	2	2	2
space group	$P2_1/c$	$P\bar{1}$	$P2_1/c$	$P\bar{1}$
λ (Mo Kα) (Å)	0.71073	0.71073	0.71073	0.71073
T (K)	150(1)	150(1)	150(1)	150(1)
ρ_{calc} (g cm^{-3})	3.80	3.65	3.36	4.87
μ (cm^{-1})	231.7	214.4	191.4	317.8
total unique data	5273	6603	5039	11978
observed data[a]	1097	1218	892	1752
refined params	97	190	100	302
$R(F)$[b]	0.0542	0.0805	0.0364	0.0612
$R_w(F)$[c]	0.0679	0.1011	0.0465	0.0819

[a] $I > 5\sigma(I)$ after data merging. [b] $R = \Sigma||F_o| - |F_c||/\Sigma|F_o|$. [c] $R_w = [\Sigma w(|F_o| - |F_c|)^2/\Sigma w|F_o|^2]^{1/2}$.

Table 2. Fractional Atomic Coordinates and Thermal Factors for $(H_3N(CH_2)_3NH_3)U_2F_{10}\cdot 2H_2O$ (UFO-1)

atom	x/a	y/b	z/c	U_{eq}[a]
U1	0.05151(7)	−0.1547(1)	0.82962(8)	0.0012(3)
F1	0.105(1)	−0.474(2)	0.798(1)	0.010(2)
F2	0.254(1)	−0.169(2)	0.843(2)	0.021(3)
F3	0.107(1)	0.076(2)	1.016(2)	0.015(3)
F4	0.084(1)	−0.201(2)	0.573(1)	0.009(2)
F5	−0.114(1)	−0.359(2)	0.772(1)	0.011(3)
N1	0.287(3)	0.388(5)	1.014(4)	0.056(8)
C1	0.5000	0.5000	1.0000	0.04(1)
C2	0.387(5)	0.51(1)	1.08(1)	0.09(3)
C3	0.402(7)	0.38(2)	0.94(1)	0.20(7)
O1	0.365(4)	0.578(7)	0.638(5)	0.12(1)

[a] U_{eq} (Å^2) = $1/3[U_{11} + U_{22} + U_{33}]$.

Table 3. Fractional Atomic Coordinates and Thermal Factors for $(H_3N(CH_2)_4NH_3)U_2F_{10}\cdot 3H_2O$ (UFO-2)

atom	x/a	y/b	z/c	U_{eq}[a]
U1	−0.3059(2)	0.0491(2)	0.6581(3)	0.0074(7)
U2	0.1943(2)	0.0490(2)	0.8515(3)	0.0063(8)
F1	−0.035(3)	0.078(3)	0.704(5)	0.017(7)
F2	−0.244(4)	0.106(3)	0.969(5)	0.028(8)
F3	0.038(3)	0.101(2)	1.083(4)	0.008(6)
F4	−0.336(3)	−0.114(3)	0.845(4)	0.013(6)
F5	−0.248(3)	−0.092(3)	0.455(4)	0.012(6)
F6	0.276(4)	0.239(3)	0.843(5)	0.021(7)
F7	−0.463(4)	0.099(3)	0.438(5)	0.019(7)
F8	−0.233(4)	0.235(3)	0.676(5)	0.028(8)
F9	−0.534(4)	0.076(3)	0.810(5)	0.020(7)
F10	−0.174(3)	0.107(3)	0.354(4)	0.013(6)
N1	0.141(6)	0.260(5)	0.365(8)	0.03(1)
N2	0.647(6)	0.256(5)	0.178(9)	0.03(1)
C1	0.606(6)	0.346(5)	0.296(9)	0.02(1)
C2	0.75(1)	0.428(8)	0.33(1)	0.05(2)
C3	0.276(6)	0.453(5)	0.552(8)	0.02(1)
C4	0.12(1)	0.358(9)	0.50(2)	0.06(3)
O1	−0.414(6)	0.362(5)	0.818(8)	0.05(1)
O2	−0.235(7)	0.589(5)	0.926(9)	0.05(2)
O3	−0.07(1)	0.376(9)	0.98(1)	0.12(3)

[a] U_{eq} (Å^2) = $1/3[U_{11} + U_{22} + U_{33}]$.

Table 4. Fractional Atomic Coordinates and Thermal Factors for $(H_3N(CH_2)_6NH_3)U_2F_{10}\cdot 2H_2O$ (UFO-3)

atom	x/a	y/b	z/c	U_{eq}[a]
U1	0.95504(5)	−0.15836(9)	1.14945(8)	0.0097(3)
F1	1.0934(7)	−0.362(1)	1.258(1)	0.020(4)
F2	0.7892(7)	−0.173(1)	1.070(1)	0.015(4)
F3	1.0856(7)	−0.078(1)	1.047(1)	0.015(3)
F4	0.9253(7)	−0.201(1)	1.393(1)	0.016(3)
F5	0.9157(7)	−0.481(1)	1.166(1)	0.016(3)
O1	0.701(1)	−0.054(2)	0.759(2)	0.041(5)
N1	1.232(1)	−0.343(3)	1.099(2)	0.029(6)
C1	1.477(1)	−0.522(3)	1.412(2)	0.029(6)
C2	1.329(1)	−0.447(3)	1.157(2)	0.023(6)
C3	1.378(1)	−0.404(3)	1.328(2)	0.017(7)

[a] U_{eq} (Å^2) = $1/3[U_{11} + U_{22} + U_{33}]$.

products were recovered by suction filtration, washed with water and tetrahydrofuran (THF), and allowed to dry in air.

Magnetic Susceptibility. Magnetic measurements were performed using a Quantum Design MPMS-5 SQUID magnetometer. Powdered samples (~20 mg) were loaded in gelatine capsules and introduced into the magnetometer using nonmagnetic straws. Diamagnetic contributions from core electrons were corrected for using Pascal constants. Data were collected employing fields of 0.2 and 0.5 T over a range 5 to 300 K.

Results and Discussion

UFO-1, UFO-2, UFO-3, and UFO-4 crystallize in the space groups $P2_1/c$, $P\bar{1}$, $P2_1/c$, and $P\bar{1}$, respectively. Selected crystallographic data for each compound are given in Table 1. Fractional atomic coordinates and thermal parameters are reported in Tables 2−5, and a list of pertinent bond lengths are given in Tables 6−9.

UFO-1−3 form a structurally related series of compounds. All three materials are layered and contain negatively charged uranium fluoride layers separated by charge-balancing $[H_3N(CH_2)_nNH_3]^{2+}$ cations and occluded water molecules. Figure 1a, b, and c shows the structures of UFO-1, UFO-2, and UFO-3, respectively, viewed along the [010] direction, and shows the layer structure of the three materials and location of the occluded template in each compound. (The occluded water molecules are omitted for clarity.) The uranium fluoride sheets are stacked along the [100] direction in each case. In all three materials, the $[H_3N(CH_2)_nNH_3]^{2+}$ cations lie almost perpendicular to the uranium fluoride

Table 5. Fractional Atomic Coordinates and Thermal Factors for $(HN(CH_2CH_2NH_3)_3)U_5F_{24}$ (UFO-4)

atom	*x*/*a*	*y*/*b*	*z*/*c*	U_{eq}[a]
U1	0.8864(2)	−0.5172(2)	0.3130(3)	0.0050(5)
U2	0.5669(2)	−0.6984(2)	0.1259(3)	0.0050(5)
U3	0.6547(2)	−0.2953(2)	0.2468(3)	0.0048(5)
U4	0.9851(2)	−0.1435(2)	0.5847(3)	0.0056(5)
U5	0.7107(2)	0.0046(2)	0.1505(3)	0.0056(5)
F1	0.549(3)	−0.705(3)	−0.119(4)	0.010(7)
F2	0.785(3)	−0.172(3)	0.173(4)	0.008(7)
F3	0.692(3)	0.159(3)	0.045(4)	0.014(7)
F4	0.865(4)	−0.168(4)	0.725(5)	0.03(1)
F5	0.541(3)	−0.120(3)	0.012(4)	0.017(8)
F6	0.383(3)	−0.667(4)	0.013(5)	0.026(9)
F7	0.617(2)	−0.092(3)	0.295(3)	0.002(6)
F8	0.593(3)	−0.852(3)	0.252(4)	0.011(7)
F9	0.548(3)	−0.283(3)	0.412(4)	0.018(8)
F10	0.913(3)	−0.494(3)	0.567(4)	0.011(7)
F11	0.981(3)	−0.310(3)	0.406(4)	0.016(8)
F12	0.465(3)	−0.663(3)	0.299(4)	0.013(7)
F13	0.980(3)	0.057(4)	0.606(5)	0.026(9)
F14	0.999(3)	−0.535(4)	0.150(5)	0.021(8)
F15	0.754(3)	−0.074(3)	−0.063(4)	0.012(7)
F16	0.751(3)	−0.619(3)	0.100(4)	0.018(8)
F17	0.716(2)	−0.627(3)	0.334(3)	−0.003(6)
F18	0.810(3)	−0.384(3)	0.171(4)	0.010(7)
F19	1.185(3)	−0.110(3)	0.604(4)	0.011(7)
F20	1.069(3)	−0.287(3)	0.693(4)	0.013(7)
F21	0.567(3)	−0.495(3)	0.185(4)	0.019(8)
F22	0.796(3)	−0.160(3)	0.457(4)	0.011(7)
F23	0.746(3)	−0.399(3)	0.409(4)	0.006(6)
F24	1.087(3)	−0.050(4)	0.816(5)	0.024(9)
N1	0.772(5)	−0.777(5)	−0.216(7)	0.02(1)
N2	1.086(4)	−0.736(5)	0.038(6)	0.01(1)
N3	0.630(4)	−0.549(5)	−0.384(7)	0.02(1)
N4	0.367(5)	−0.905(6)	0.331(7)	0.03(1)
C1	0.908(5)	−0.726(6)	−0.142(7)	0.02(1)
C2	0.967(4)	−0.793(5)	−0.031(6)	0.01(1)
C3	0.725(5)	−0.709(6)	−0.333(8)	0.02(1)
C4	0.717(6)	−0.590(7)	−0.257(9)	0.02(2)
C5	0.757(5)	−0.914(6)	−0.267(8)	0.02(1)
C6	0.636(6)	−0.967(7)	−0.316(9)	0.02(2)

[a] U_{eq} (Å^2) $= 1/3[U_{11} + U_{22} + U_{33}]$.

Table 6. Selected Bond Distances for $(H_3N(CH_2)_3NH_3)U_2F_{10}\cdot 2H_2O$ (UFO-1)

bond	distance, Å	bond	distance, Å
U(1)−F(1)	2.359(8)	U(1)−F(5)[a]	2.394(8)
U(1)−F(1)[a]	2.334(7)	N(1)−C(2)	1.44(4)
U(1)−F(2)	2.17(1)	N(1)−C(3)	1.43(5)
U(1)−F(3)	2.347(8)	C(1)−C(2)	1.43(4)
U(1)−F(3)[a]	2.326(8)	C(1)−C(2)	1.43(4)
U(1)−F(4)	2.316(8)	C(1)−C(3)	1.45(5)
U(1)−F(4)[a]	2.380(8)	C(1)−C(3)	1.45(5)
U(1)−F(5)	2.321(8)		

[a] Symmetry equivalent atoms.

layers, at angles of ∼90°, 85°, and 75° for $n = 3$, 4, and 6, respectively. Hence, as the size of the organic cation increases, the interlayer separation also steadily increases. The interlayer separations are 10.7, 11.5, and 13.1 Å, respectively. The layers are bound together by the ionic bonding between the $[H_3N(CH_2)_nNH_3]^{2+}$ cations and the negatively charged $U_2F_{10}{}^{2-}$ layers, and by a complex network of strong hydrogen bonds between the substituted ammonium groups and the fluorine atoms of the layers, the oxygen atoms of the water molecules and the fluorines, and the ammonium groups and the water molecules.

Table 7. Selected Bond Distances for $(H_3N(CH_2)_4NH_3)U_2F_{10}\cdot 3H_2O$ (UFO-2)

bond	distance, Å	bond	distance, Å
U(1)−F(1)	2.32(2)	U(2)−F(3)[a]	2.33(2)
U(1)−F(2)	2.34(2)	U(2)−F(4)	2.45(2)
U(1)−F(4)	2.35(2)	U(2)−F(5)	2.31(2)
U(1)−F(5)	2.34(2)	U(2)−F(6)	2.19(2)
U(1)−F(7)	2.33(2)	U(2)−F(9)	2.32(2)
U(1)−F(7)[a]	2.34(2)	U(2)−F(10)	2.32(2)
U(1)−F(8)	2.14(3)	N(1)−C(4)	1.47(8)
U(1)−F(9)	2.38(2)	N(2)−C(1)	1.47(6)
U(1)−F(10)	2.47(2)	C(1)−C(2)	1.36(8)
U(2)−F(1)	2.39(2)	C(2)−C(3)	1.64(8)
U(2)−F(2)	2.42(2)	C(3)−C(4)	1.57(8)
U(2)−F(3)	2.33(2)		

[a] Symmetry equivalent atoms.

Table 8. Selected Bond Distances for $(H_3N(CH_2)_6NH_3)U_2F_{10}\cdot 2H_2O$ (UFO-3)

bond	distance, Å	bond	distance, Å
U(1)−F(1)	2.340(6)	U(1)−F(5)	2.351(6)
U(1)−F(1)[a]	2.414(6)	U(1)−F(5)[a]	2.347(6)
U(1)−F(2)	2.168(6)	N(1)−C(2)	1.51(2)
U(1)−F(3)	2.321(6)	C(1)−C(1)	1.49(2)
U(1)−F(3)[a]	2.336(6)	C(1)−C(3)	1.54(2)
U(1)−F(4)	2.314(6)	C(2)−C(3)	1.46(2)
U(1)−F(4)[a]	2.349(6)		

[a] Symmetry equivalent atoms.

Table 9. Selected Bond Distances for $(HN(CH_2CH_2NH_3)_3)U_5F_{24}$ (UFO-4)

bond	distance, Å	bond	distance, Å
U(1)−F(10)	2.33(2)	U(3)−F(23)	2.34(2)
U(1)−F(10)[a]	2.39(2)	U(4)−F(4)	2.16(3)
U(1)−F(11)	2.41(3)	U(4)−F(11)	2.28(3)
U(1)−F(14)	2.20(2)	U(4)−F(13)	2.30(3)
U(1)−F(16)	2.35(2)	U(4)−F(13)[a]	2.39(3)
U(1)−F(17)	2.35(2)	U(4)−F(19)	2.30(2)
U(1)−F(18)	2.38(2)	U(4)−F(20)	2.33(2)
U(1)−F(20)	2.34(3)	U(4)−F(22)	2.27(2)
U(1)−F(23)	2.35(2)	U(4)−F(24)	2.31(2)
U(2)−F(1)	2.31(2)	U(5)−F(2)	2.29(2)
U(2)−F(3)	2.40(2)	U(5)−F(3)	2.25(3)
U(2)−F(5)	2.31(2)	U(5)−F(5)	2.31(2)
U(2)−F(6)	2.31(2)	U(5)−F(7)	2.34(2)
U(2)−F(8)	2.42(2)	U(5)−F(8)	2.33(2)
U(2)−F(12)	2.17(2)	U(5)−F(15)	2.20(2)
U(2)−F(16)	2.37(2)	U(5)−F(19)	2.38(2)
U(2)−F(17)	2.33(2)	U(5)−F(24)	2.31(2)
U(2)−F(21)	2.30(2)	N(1)−C(1)	1.60(5)
U(3)−F(1)	2.45(2)	N(1)−C(3)	1.57(5)
U(3)−F(2)	2.35(2)	N(1)−C(5)	1.49(6)
U(3)−F(6)	2.36(3)	N(2)−C(2)	1.42(5)
U(3)−F(7)	2.36(2)	N(3)−C(4)	1.53(5)
U(3)−F(9)	2.19(3)	N(4)−C(6)	1.45(7)
U(3)−F(18)	2.29(2)	C(1)−C(2)	1.57(6)
U(3)−F(21)	2.31(2)	C(3)−C(4)	1.45(6)
U(3)−F(22)	2.44(2)	C(5)−C(6)	1.49(6)

[a] Symmetry equivalent atoms.

The structure of the individual uranium fluoride layers is essentially identical in each of the three materials. Figure 2a shows the structure of a single layer in UFO-1 viewed perpendicular to the layer (along the [100] direction). Each unique uranium atom (there is only one unique uranium in UFO-1 and UFO-3, two in UFO-2) is bonded to nine fluorine atoms in a tricapped trigonal prismatic coordination. The local geometry around each uranium is shown in Figure 2b. A similar uranium coordination geometry has been observed in condensed uranium fluorides such as β-NH_4UF_5,[66] $LiUF_5$,[67] and $K_2U_2F_9$.[68] Equivalent UF_9 polyhe-

---

(66) Penneman, R. A.; Ryan, R. R. *Acta Crystallogr.* **1974**, *B30*, 1966.

(67) Brunton, G. *Acta Crystallogr.* **1966**, *21*, 814.

(68) Brunton, G. *Acta Crystallogr.* **1969**, *B25*, 1919.

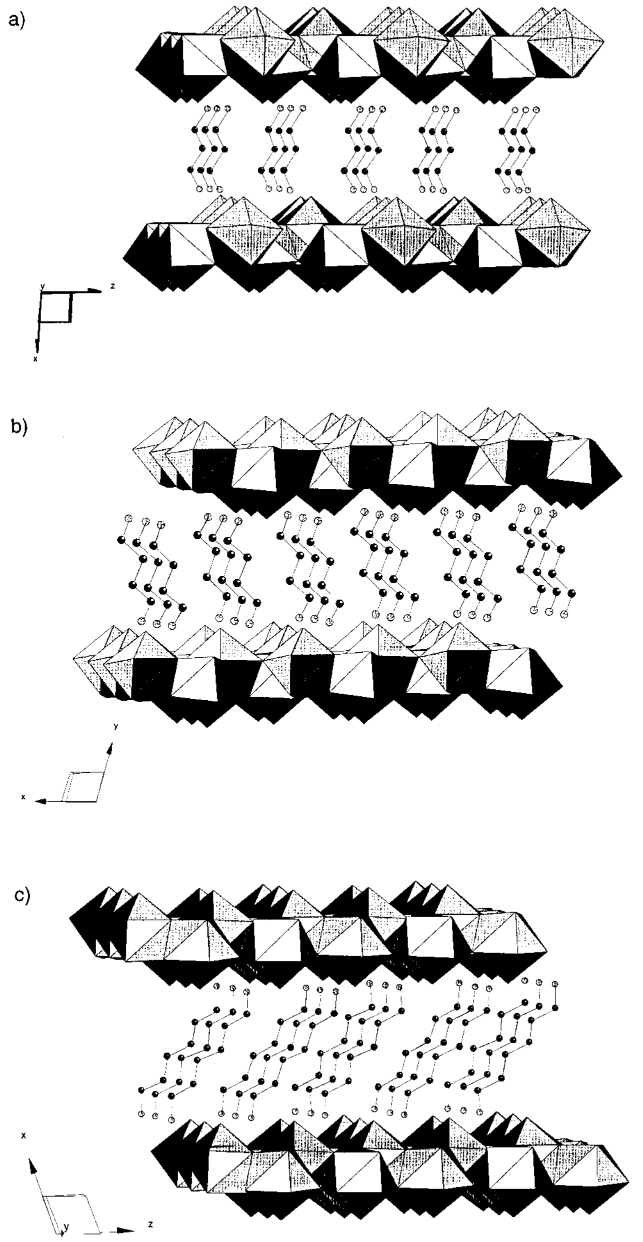

Figure 1. The structure of (a) $(H_3N(CH_2)_3NH_2)U_2F_{10}\cdot 2H_2O$ (UFO-1), (b) $(H_3N(CH_2)_4NH_2)U_2F_{10}\cdot 3H_2O$ (UFO-2), and (c) $(H_3N(CH_2)_6NH_2)U_2F_{10}\cdot 2H_2O$ (UFO-3) viewed parallel to the uranium fluoride layers (along the [010] direction) showing the location of the organic template in each case. The carbon atoms are represented by dark spheres, the nitrogen atoms by lighter spheres. The occluded water molecules are excluded for clarity. In UFO-1, the $(H_3N(CH_2)_3NH_3)^{2+}$ cation lies on an inversion center and the end carbon atom is disordered around this position. For clarity, this disorder is not represented in the figure and only one orientation of the template is shown.

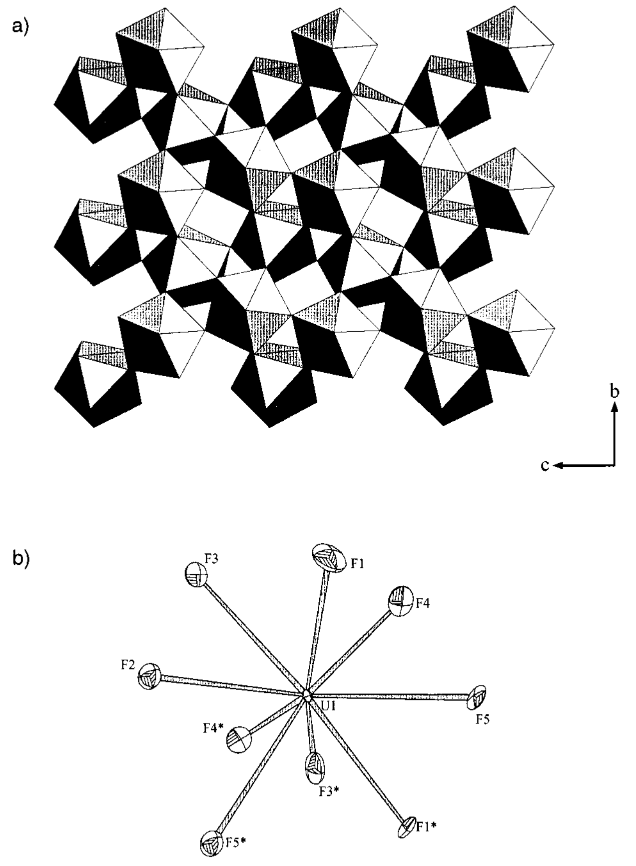

Figure 2. (a) The structure of a single uranium fluoride layer of $(H_3N(CH_2)_3NH_2)U_2F_{10}\cdot 2H_2O$ (UFO-1) viewed perpendicular to the layers (along the [100] direction) showing how the layers are constructed from edge and corner sharing $[UF_9]$ tricapped trigonal prisms. $(H_3N(CH_2)_4NH_2)U_2F_{10}\cdot 3H_2O$ (UFO-2) and $(H_3N(CH_2)_6NH_2)U_2F_{10}\cdot 2H_2O$ (UFO-3) contain essentially identical layers. (b) A view of the local coordination around each uranium atom.

dra share three edges with three adjacent polyhedra and share two corners with two additional polyhedra to form uranium fluoride sheets. The ninth fluorine atom of each polyhedra is terminal and projects out of the layers and toward adjacent sheets, and is strongly hydrogen bonded to the interlamellar organic cation. The U−F bond involving the terminal fluorine atom is significantly shorter than the other U−F bonds. Averaged over UFO-1, 2, and 3, the mean U−F distance for a terminal fluorine is 2.16 Å (ranging between 2.13 and 2.18 Å), whereas for the bridging fluorines, the mean U−F distance is 2.35 Å (ranging between 2.28 and 2.44 Å). The identical nature of the layers in each case is reflected in the fact that two of the lattice parameters are almost identical for each compound (see Table 1).

UFO-4 is also a layered material containing negatively charged sheets that are of generally similar structure to those of the materials just discussed but with some small differences. There are five unique uranium atoms in the asymmetric unit. Three of these are bonded to nine fluorine atoms in a distorted tricapped trigonal prismatic coordination similar to that seen in UFO-1−3, whereas the other two are coordinated to eight fluorine atoms in a distorted bicapped trigonal prismatic coordination. Each of the UF_9 polyhedra share three edges and two corners with adjacent polyhedra, whereas the UF_8 polyhedra share two edges and three corners. Figure 3 is a view of UFO-4 along the [10-1] direction and shows the structure of a single $[U_5F_{24}]_n^{4n-}$ layer and emphasizes the rather complex nature of the layers. Although the structure of the uranium fluoride sheets is similar to those seen in $(H_3N(CH_2)_nNH_3)U_2F_{10}\cdot xH_2O$, the presence of the eight coordinated uranium atoms leads to some subtle differences, as can be seen from a comparison of Figures 3 and 2. Each uranium atoms is bonded to an unshared, terminal fluorine atom that projects above and below the plane of the layers. The U−F bond distance to the

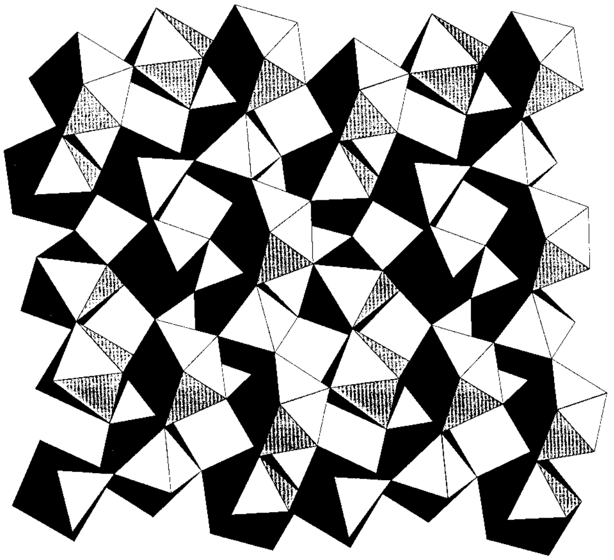

Figure 3. The structure of $[HN(CH_2CH_2NH_3)_3]U_5F_{24}$ (UFO-4) viewed along the [10-1] direction (perpendicular to the uranium fluoride layers) showing a single $[U_5F_{24}]_n^{4n-}$ layer.

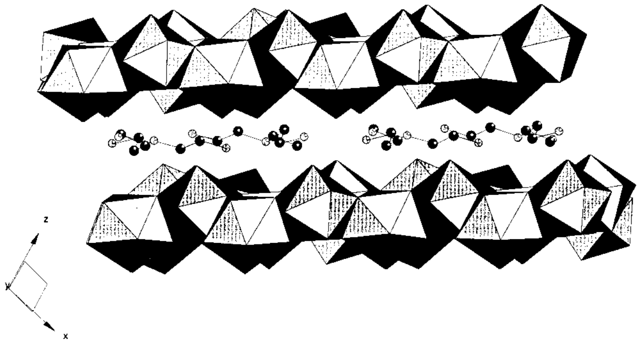

Figure 4. A view of the structure of UFO-4 along the [010] direction (parallel to the layers), showing the location of the occluded template. The carbon atoms are represented by dark spheres, the nitrogen atoms by lighter spheres.

terminal fluorine is significantly shorter than the bond distance to the bridging fluorine atoms ($U-F_T$ (av) = 2.20 Å, $U-F_{Br}$ (av) = 2.33 Å).

The uranium fluoride sheets stack along the [10-1] direction and are separated by charge-balancing $(HN(CH_2CH_2NH_3)_3)^{4+}$ cations. The interlayer separation is 11.5 Å. The cations reside in an almost flat conformation with the 2-aminoethyl chains lying almost parallel to the plane of the uranium fluoride layers. Figure 4 is a view of the structure of UFO-4 along the [010] direction, and shows the location of the occluded template. A complex network of strong hydrogen bonds between all of the nitrogens of the $(HN(CH_2CH_2NH_3)_3)^{4+}$ cations and the fluorine atoms in the layers bind the layers together.

Thermogravimetric Analysis (TGA). The thermal behavior of the materials was investigated using TGA and differential scanning calorimetry (DSC). Each of the four materials exhibited similar behavior. When the materials are heated in air, all four materials undergo a weight loss of 5−8% between room temperature and 200 °C that is attributed to the loss of the occluded water from the materials. Between the temperatures of ~220 and 350 °C, the materials undergo a more substantial weight loss of ~10%, 11%, and 14% for UFO-1, UFO-2, and UFO-3, respectively, which can be attributed to the combustion of the template and its loss from the materials. Immediately following this, a further weight loss of ~15% begins that presumably corresponds to decomposition of the uranium fluoride layers. Powder X-ray diffraction (XRD) confirmed that this weight loss is associated with a loss in crystallinity of the materials. Elemental analysis confirmed that the calcined products contained only trace amounts of carbon and nitrogen indicating total decomposition of the templates. The initial loss of occluded water is fully reversible; if the materials are heated to 165 °C, then cooled back down to room temperature and allowed to stand in atmospheric air, complete rehydration occurs within an hour.

When heated in flowing nitrogen, the materials exhibited behavior similar to that in air. Powder XRD of the materials after heating to 800 °C in nitrogen again indicated that the materials were amorphous, and elemental analysis again showed that template loss had occurred.

Ion-Exchange Experiments. The charged frameworks and large interlayer separations present in these materials suggested that they may be able to undergo ion-exchange reactions in which the organic template is replaced by other cationic species. These experiments revealed that UFO-1, 2, and 3 display robust ion-exchange behavior. (The ion-exchange properties of UFO-4 were not investigated because of the presence of impurity phases in the as synthesized product.) It was possible to completely exchange the organic template for Na^+, K^+, Cs^+, and Co^{2+} simply by stirring suspensions of the host materials in ~2 M solutions of the appropriate metal salts for 1−4 days at room temperature (or 70 °C in the case of Co^{2+}). In each case, powder XRD of the ion-exchanged materials indicated that all are highly crystalline, and the exchange is accompanied by a large decrease in interlayer spacing. The interlayer separation decreases to 7.5 Å, 8.1, 7.2, and 11.0 Å for the Na^+, K^+, Cs^+, and Co^{2+} exchanged materials, respectively. The rather small decrease in the interlayer separation in the Co^{2+} exchanged material suggests the possibility of a bilayer structure in which the crystallographic repeat distance in the direction perpendicular to the layers is twice the interlayer separation.

Powder XRD revealed that the exchange of any particular cation with all three host materials yielded identical products. In the case of the potassium exchanged material, the diffraction pattern matched that of a reported material '$K_7U_6F_{31}$'. The powder XRD pattern of this material is shown in Figure 5. However, although a cell and space group were given in the original report, no structural data were reported. Given the mild synthetic route that we employed to synthesize this material, we believe the empirical formula is more likely to be $KUF_5{\cdot}xH_2O$ ('$K_6U_6F_{30}$'), because the formation of $K_7U_6F_{31}$ would appear to require a fairly substantial structural reorganization. A full ab initio structural determination using powder data is in progress to confirm the identity of this phase. The powder XRD patterns of the exchanged materials with other cations did not match any known phases, indicating that the ion-exchange of UFO-1, 2, and 3 provides a facile route

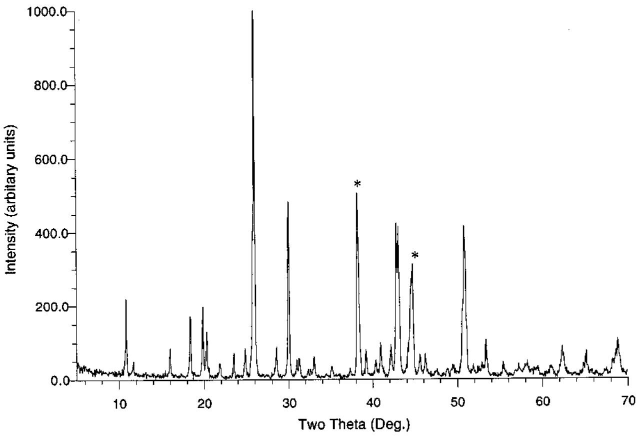

Figure 5. Powder X-ray diffraction pattern (Cu Kα radiation) of the product of ion-exchange of UFO-3 with K^+ ions. (Peaks labeled * correspond to reflections from the aluminum sample holder.)

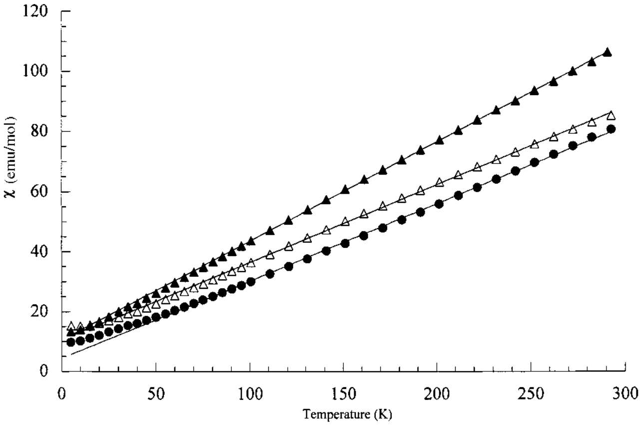

Figure 6. Plot of the variation of inverse molar magnetic susceptibility with temperature for $(H_3N(CH_2)_3NH_2)U_2F_{10}\cdot 2H_2O$ (UFO-1), $(H_3N(CH_2)_4NH_2)U_2F_{10}\cdot 3H_2O$ (UFO-2), and $(H_3N(CH_2)_6NH_2)U_2F_{10}\cdot 2H_2O$ (UFO-3) at a magnetic field of 0.5 T. (●) UFO-1, (▲) UFO-2, (△) UFO-3.

for the low temperature synthesis of new alkali metal and transition metal uranium(IV) fluorides. Work is currently underway to confirm the phase purity of these materials, and to determine their structures.

Magnetic Measurements. The magnetic behavior of phases UFO-1−3 was investigated. The magnetic susceptibilities of powdered samples of each material were measured over the temperature range 5−300 K in magnetic fields of 0.2 and 0.5 T. The variation of the magnetic susceptibilities with temperature of the three materials is displayed in Figure 6.

Over the temperature range 20−300 K, all three materials displayed magnetic susceptibilities that could be fitted well to the simple Curie−Weiss equation (susceptibility, $\chi_{\mathrm{mol}} = C/(\mathrm{T} - \Theta)$). Below 20 K, there is slight leveling off of the magnetic susceptibility, a feature that was most marked for UFO-3 (see Figure 6). This result is indicative of either very weak antiferromagnetic ordering between U^{4+} ions or temperature-dependent paramagnetism due to changing populations of atomic energy levels of individual U^{4+} ions. Fitting of the high temperature (>20 K) $1/\chi_{\mathrm{mol}}$ against T data to the Curie−Weiss equation using a least-squares routine yielded values for the Curie and Weiss constants for each of the three compounds. In each case, negative values of the Weiss constant were obtained, which is consistent with weak antiferromagnetism. Curie constants of 4.01, 3.01, and 3.88 emu K mol^{-1} were obtained for UFO-1, 2, and 3, respectively, which yields values of μ_{eff} of 5.66, 4.91, and 5.57 μ_B, respectively. These values are somewhat higher than would be expected for U(IV) ions. However, interpreting effective magnetic moments of uranium compounds is very complex because spin−spin, orbit−orbit, spin−orbit, and ligand−field interactions are all of comparable importance and must all be considered in a full treatment. The values of C, Θ, and μ_{eff} for each compound are detailed in Table 10.

Table 10. Values of the Curie Constant, Weiss Constant, and Effective Magnetic Moment for $(H_3N(CH_2)_nNH_3)U_2F_{10}\cdot xH_2O$[a]

compound	C (emu K mol^{-1})	Θ (K)	μ_{eff} (m_B)
$(H_3N(CH_2)_3NH_3)U_2F_{10}\cdot 2H_2O$ (●)	4.01(3)	−24.7(13)	5.66
$(H_3N(CH_2)_4NH_3)U_2F_{10}\cdot 3H_2O$ (▲)	3.01(1)	−30.9(4)	4.91
$(H_3N(CH_2)_6NH_3)U_2F_{10}\cdot 2H_2O$ (△)	3.88(12)	−41.7(11)	5.57

[a] $n = 3, 4, 6$; $x = 2, 3$; obtained by fitting of the susceptibility data shown in Figure 6 to the Curie−Weiss law, $C = \chi/(\mathrm{T} - \Theta)$, where $C = N\mu_B{}^2\mu_{\mathrm{eff}}{}^2/3k$.

Conclusion/Summary

In summary, we have outlined a simple, high-yield, single-step route to the exclusive synthesis of the first examples of a new class of hybrid inorganic/organic uranium(IV) fluorides, and demonstrated how organically templated hydrothermal synthesis can be successfully exploited to synthesize novel uranium-containing phases in which the organic template is incorporated into the inorganic framework. These materials are the first purely flourinated compounds synthesized via template-mediated hydrothermal synthesis. The materials reversibly dehydrate when heated, display weak antiferromagnetic properties, and undergo facile ion-exchange reactions with a variety of other cations leading to the low temperature formation of new condensed uranium(IV) phases. Structurally, the phases $(H_3N(CH_2)_nNH_3)U_2F_{10}\cdot xH_2O$ (where $n = 3$, 4, or 6; i.e., UFO-1, 2, and 3, respectively) contain inorganic layers of an identical nature, but the different structure and stoichiometry of the layers in UFO-4 show how the nature of the final phase can be subtly controlled by the use of structure-directing species of different size, shape, and charge distribution.

Although the number of templating species used to date is fairly small, initial studies suggest that the formation of these phases is quite a general reaction. Time-resolved in situ powder XRD experiments that we have performed during the hydrothermal syntheses of these materials, using the experimental apparatus that we previously reported,[69] showed that at the reaction temperature (180 °C) there are no solid crystalline phases present, and the reported product only crystallizes as the reaction mixtures are cooled (in situ diffraction data showed that the products began to form at ~120−130 °C). Given the huge variety of possible

---

[69] Evans, J. S. O.; Francis, R. J.; O'Hare, D.; Price, S. J.; Clarke, S. M.; Flaherty, J.; Gordon, J.; Nield, A.; Tang, C. C. *Rev. Sci. Instrum.* **1995**, *66*, 2442.

templates that could be used, both purely organic and otherwise, this result suggests that hydrothermal crystallizations of these type will provide a versatile and facile synthetic route to the formation of a wide variety of novel materials.

Of particular interest in this regard is the contrast between the fairly rigid pentagonal bipyramidal coordination seen in the organically templated uranium(VI) phosphates previously reported[41] and the more flexible coordination displayed in these phases. Indeed, in previously known uranium fluoride phases, a variety of six, seven, eight, and nine uranium coordination geometries have been observed. Hence, although the materials reported here have all been layered phases, these systems appear to offer great promise for the synthesis of other structure types, including three-dimensional open-framework uranium-containing phases, via the judicious choice of the correct templating species and reaction conditions. Indeed, we have been exploring the synthesis of other materials using a variety of other templating species and have recently isolated a one-dimensional chain structure, which to our knowledge has an unprecedented structure type for uranium(IV) fluorides.[70] Using the same template under somewhat different conditions, we have also been successful in synthesising a ‘molecular’ phase containing isolated uranium fluoride dimers.[70] Thus it appears that the connectivity of uranium fluoride linkages can be systematically controlled via the subtle control of the precise reaction conditions, increasing the possibilities for the synthesis of uranium-containing materials with desirable structural, catalytic, ion-exchange, and magnetic properties

Acknowledgment. We thank British Nuclear Fuels Limited, the Leverhulme Fund, and EPSRC for financial support. P.S.H. thanks Christ Church, Oxford, for a Junior Research Fellowship.

Supporting Information Available: X-ray structural data for UFO-1, UFO-2, UFO-3, and UFO-4, including a summary of crystallographic parameters, atomic coordinates, bond distances and angles, and isotropic and anisotropic thermal parameters (29 pages). Tables of structure factors (64 pages). Ordering information is given on any current masthead page.

CM980225X

---

[70] Francis, R. J.; Halasyamani, P. S.; Bee, J.; O'Hare, D., unpublished results.